LOWLAND TECHNOLOGY INTERNATIONAL SI, Vol. 9, No. 2, 49-55, December 2007
International Association of Lowland Technology (IALT), ISSN 1344-9656

SEGREGATION OF MICROPHYTOBENTHIC CHLOROPHYLL-A FROM SUSPENDED PARTICLES DURING TIDAL CYCLE IN NANAURA MUDFLAT, ARIAKE SEA, JAPAN

C.-H. Koh[1], J.S. Khim[2], H. Araki[3], H. Yamanishi[4] and K. Koga[5]

ABSTRACT: The fluxes of microphytobenthic chlorophyll *a* (Chl-*a*) and suspended particulate matter (SPM) in water column and their relationship against tidal current have been examined during 15-days of full spring-neap tidal periods in the upper intertidal flat of Nanaura, Saga, Ariake Sea, Japan. The flood-ebb and spring-neap tidal conditions influenced within-day and daily variability in the fluxes of Chl-*a* and SPM, in terms of tidal energy. The Chl-*a* flux decreased relatively at slower pace than corresponding SPM flux at stage of decelerating incoming tide, which indicated the segregation of Chl-*a* from SPM followed by the slower settlement at depositional period. This 'decoupling' trend was consistently observed during the high tidal energy period of spring, particularly during the lower wind period (0-1 m s^{-1}), but this was no more prevalent during the low tidal energy of neap and/or higher wind period (3-5 m s^{-1}).

Keywords: Buoyancy, microphytobenthos, suspended particulate matter, tidal flat

INTRODUCTION

Resuspension and sedimentation of suspended particulate matter (SPM) in coastal areas have well been studied to understand the general features of sediment transport and dynamics in water column during the last decades (Kuehl et al. 1996; Black 1998; Widdows et al. 2004). Since those earlier studies mainly concerned with transport and deposition, focuses were SPM itself, thus little attention has been paid as for understanding phyto-particles such as plankton and microphytobenthos. Particle size was considered as a key factor in determining the buoyancy, transport and deposition of sediment in coastal zone.

Meanwhile, several studies performed to address physical movement of some phytoplankton (Smayda 1974). Those studies also addressed the dynamics of floating and sinking in terms of size and shape, and species specific behavior in buoyancy have been described in that aspect. In the water column of tidal flat area, however, phyto-particles occur highly together with SPM due to the large biomass of microphytobenthos on fine mud sediments; the Nanaura tidal flat showed a ratio of ca 1:1000 (Koh et al. 2006).

Microphytobenthos belongs to the size group of mud particles and resuspended with mud particles into water column during flood (Koh et al. 2006). The similar size of microphytobenthos allows us to expect similar buoyancy with SPM in a highly dynamic tidal flat environment. In the present study, however, we tried to describe the behavior in buoyancy of phyto-particles separately from SPM.

Recently, we reported the close relationship between the amount of SPM and microphytobenthos biomass, namely total Chl-*a*, in water column during 28 consecutive tidal cycles (Koh et al. 2006). Particularly, the ratio of Chl-*a* / SPM indicated the different floating / sinking behavior of those particle groups during the course of tidal cycle. The behavioral segregation of Chl-*a* from SPM was evidenced by the decreasing Chl-*a* / SPM ratio after the mid flood tide when the current velocity was decelerated. This trend was observed based on the concentrations of total Chl-*a* and SPM in water column. In this study, we tried further to segregate the floating / sinking behavior of phyto-particles from SPM by applying an index of 'flux'. The 15-day data of the previous study was applied for the purpose.

[1] Professor, IALT member, School of Earth and Environmental Sciences, Seoul National University, Seoul 151-742, Korea
[2] Research Associate, School of Earth and Environmental Sciences, Seoul National University, Seoul 151-742, Korea
[3] Professor, IALT member, Institute of Lowland Technology, Saga University, Saga 840-8502, Japan
[4] Assoc. Professor, IALT member, Institute of Lowland Technology, Saga University, Saga 840-8502, Japan
[5] Professor, IALT member, Faculty of Science and Engineering, Saga University, Saga 840-8502, Japan
Note: Discussion on this paper is open until June 2008

METHODS

Field Measurement

The 15-day time series data was collected from the upper intertidal flat of Nanaura, Japan by use of the mooring sensor equipped with current meter (Compact-EM; Alec Electronics, Kobe, Japan) and chlorophyll-turbidity sensor (Compact-CLW; Alec Electronics). The total Chl-*a*, SPM, current velocity and direction, and water depth etc. are automatically measured at intervals of 10 min in water column during 28 tidal cycles (Mar 20-Apr 3, 2003). The wind speed data was also obtained from the Japan Meteorological Agency (JMA) at Shiroishi, near to the study site. All the measurement data was used for the flux calculation described as below. The detailed methods for the field measurement have been fully given in our earlier publication (Koh et al. 2006).

Flux Calculation

To calculate the flux of Chl-*a* and SPM in water column, first, the depth-integrated Chl-*a* (mg m^{-2}) and SPM (g m^{-2}) are determined by Eq. (1), assuming their constant vertical distribution as follows:

$$C_w(t)*h(t) \quad (1)$$

where $C_w(t)$ is the concentration of Chl-*a* (mg m^{-3}) or SPM (g m^{-3}) at time t and $h(t)$ is the time-dependent water depth (m).

Next, the Chl-*a* (g m^{-1} s^{-1}) and SPM (Kg m^{-1} s^{-1}) flux are calculated by *Eq. (2)*:

$$C_w(t)*h(t)*Vel(t) \quad (2)$$

where $C_w(t)*h(t)$ is the depth-integrated concentration of Chl-*a* (mg m^{-2}) and SPM (g m^{-2}) at time t from Eq. (1) and $Vel(t)$ is the corresponding current velocity (m s^{-1}) at time t. A direction (Dir) of tide was considered for a net flux calculation, where values of positive (+) or negative (-) indicate onshore or offshore flux, respectively (see Fig. 1). Detailed calculation procedure for the Chl-*a* and SPM flux are presented in our earlier publication (Koh et al. 2006).

Flux Description

The Chl-*a* flux is plotted against SPM flux during tidal stages of incoming-accelerating (stage-1), incoming-decelerating (stage-2), outgoing-decelerating (stage-3), and outgoing-accelerating current (stage-4), respectively. The Chl-*a* versus SPM flux relationship could be exampled by 4-representative periods in terms of tidal energy (viz. binary combination of spring or neap and high- or low-wind speed period). The resuspension and sedimentation characteristics of Chl-*a* in association with SPM are selectively described case by case to address regular (e.g., coupling, de-coupling (segregation), and flux lag) and/or irregular flux pattern of Chl-*a* and SPM.

RESULTS

Tide Characteristics

The current velocities showed great within day temporal variations ranging from 0.002 to 0.26 m s^{-1}. Within a tidal cycle, the tidal current generally showed consistent temporal pattern and characterized as follows; (1) tidal current to onshore direction accelerated and reached a maximum quickly, mostly within 30 min, at early flood (set to stage-1), (2) incoming tidal current slowly decreased down to zero (slack water period), usually in 2-3 hours, during mid to late flood period (set to stage-2), then, (3) tidal current turned to offshore direction with slow increase at early-middle of ebb again in 2-3 hours (set to stage-3), and finally (4) outgoing tidal current decelerated relatively quickly, mostly in 1-2 hours, by the end of ebb (set to stage-4).

In general, current velocities were found to be more variable during flood (mean=0.10±0.06 m s^{-1}) than ebb tide (mean=0.08±0.04 m s^{-1}), indicating more dynamic tidal conditions during the flood period. In terms of tidal strength, the spring current velocity (mean=0.12±0.05 m s^{-1}) was about twice greater than the neap current velocity (mean=0.07± 0.04 m s^{-1}), on average.

Flux Characteristics for Chl-*a* and SPM

The Chl-*a* and SPM fluxes in water column during the observation period of 28 tidal cycles are shown in Fig. 1; during the course of spring (tide #1-7) - neap (tide #8-21) - spring (tide #22-28) tide. The fluxes of Chl-*a* and SPM, on a tide basis, showed increasing and decreasing trends throughout the semi-lunar tidal period. Higher Chl-*a* and SPM fluxes during the spring tide compared to those in neap tide clearly reflected the strength of tidal energy. This spring-neap pattern of Chl-*a* and SPM flux was consistent with that of Chl-*a* and SPM concentration (i.e., without considering the current strength) as found in the earlier study (Koh et al. 2006).

Within a tidal cycle, the offshore Chl-*a* flux was generally greater than the onshore Chl-*a* flux, especially

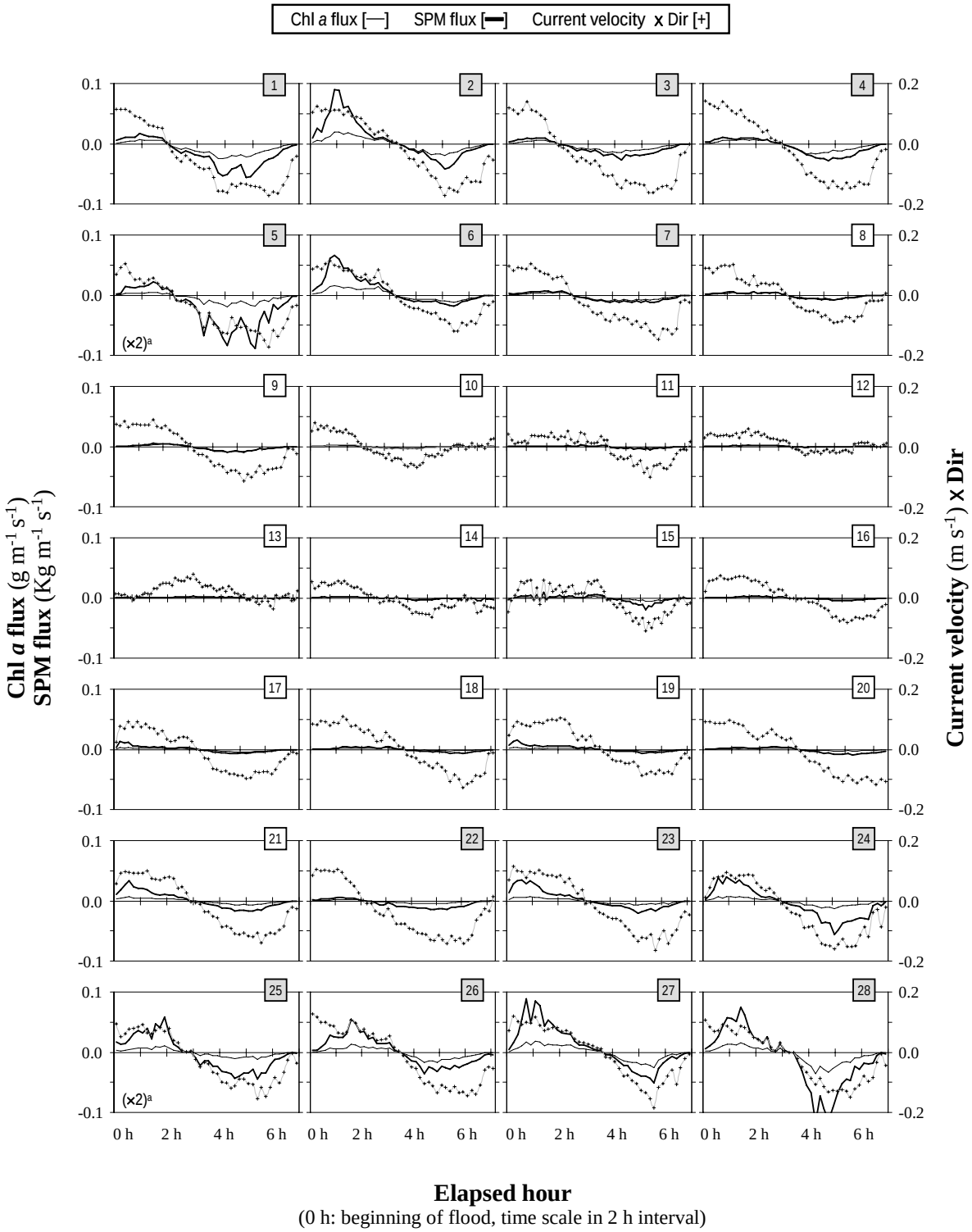

Fig. 1 Temporal changes in fluxes of chlorophyll *a* (Chl-*a*) and suspended particulate matter (SPM) in water column during submergence (28 tidal cycles), observed in the upper intertidal flat of Nanaura, Ariake Sea, Japan, corresponding current velocity (x direction) is given as well. [a]Note that Chl-*a* and SPM flux data from tide # 5 and #25 have y-axis values that are double in the scale (x 2), relative to the other panels. Numbers at the upper right of each panel: number of tidal cycle, where numbers in gray box indicate data for spring tide and in white box represent data for neap tide period

during the spring tidal period (i.e., net offshore flux was observed for 11 out of 14 spring tides, while only 6 out of 14 neap tides). The predominant offshore net flux for Chl-*a* during each tidal cycle apparently resulted in the net offshore time-integrated flux of Chl-*a* during the observation period.

Clear spring-neap variability was also observed for SPM flux within a corresponding tidal period. Similar to Chl-*a* flux, SPM flux also showed predominant daily offshore flux followed by net offshore time-integrated flux. The positive correlation between Chl-*a* and SPM flux and their similar spring-neap variation throughout the measurement period broadly supported the coupling mechanism of phyto-particles to suspended sediments in water column during the resuspension and transportation process (Koh et al. 2006).

Relationship between Chl-*a* and SPM Flux

To examine the time dependent distribution of Chl-*a* and SPM in water column, in response to the strength of tidal energy (namely current velocity and/or wind speed), the Chl-*a* flux has been compared with corresponding SPM flux during incoming (onshore) and outgoing (offshore) tidal stages, in greater detail. Previously we found that the current velocity was the most prevailing component to control the temporal distribution of suspended particles in the upper intertidal flat of Nanaura tidal flat (Koh et al. 2006). Since the Chl-*a* and SPM concentrations showed highly variable and irregular fluctuation during high wind period (usually >2 ms s^{-1}) at times, it was necessary to see the Chl-*a* and SPM flux after discriminating wind effect from current. This was done by grouping the data into 4 different tidal conditions, i.e., combination of high and low current velocity and high and low wind speed.

Clear and relatively consistent temporal trend of Chl-*a* and SPM flux are found during the low wind period as expected, and the data during these periods showed the coupling and decoupling of Chl-*a* flux from SPM. The selected examples during each condition have been presented to describe the relationship between Chl-*a* and SPM flux in terms of their interactive behaviors. Plotted data for Chl-*a* and SPM flux are described at each tidal stage of 1-4 (based on the characteristics of current velocity) to explain their fluxes and relationship between Chl-*a* and SPM in response to the tidal condition.

Flux for Group I Data

First, during the high tidal current (spring) and low wind speed (mostly 0-1 m s^{-1}) period, the Chl-*a* and SPM flux showed typical temporal trend of the coupling followed by the decoupling behavior (Fig. 2). This phenomenon has been consistently observed for 10 out of 14 spring tides. The proportional increase of both Chl-*a* and SPM flux was found in response to accelerating tidal current at stage-1 followed by flux lag and decoupling behavior of Chl-*a* from SPM at stage-2.

Although the stage-2 corresponds to a period of decelerating current velocity, the Chl-*a* and SPM flux increased for a short time (denoted as *'lag'* in Fig. 2), then slowly decreased during the last of period till slack water. Decoupling behavior could be explained by the temporal flux of Chl-*a* and SPM, where the Chl-*a* flux relatively slowly decelerated compared to SPM flux. This phenomenon pronounced mostly during the high current and low wind speed period, indicating that the segregation of microphytobenthic Chl-*a* from sediment particles (SPM) in water column is mainly controlled by the tidal current.

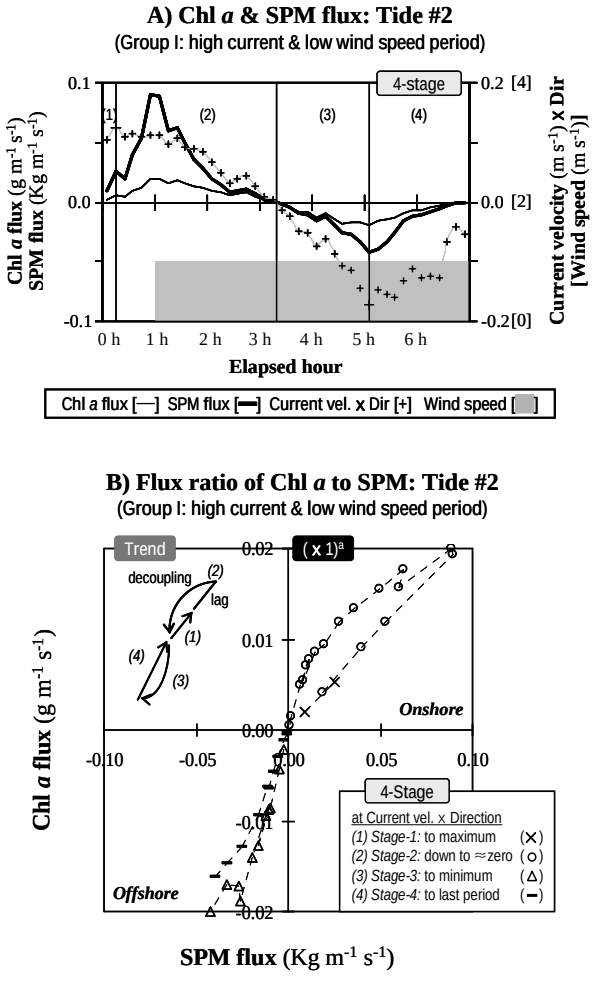

Fig. 2 Chl-*a* and SPM flux during period of high current (spring) and low wind speed (<2 m s^{-1}); example of tide #2 (categorized to Group I; tide #1, 2, 3, 4, 6, 7, 22, 23, 27, and 28), showing A) Chl-*a* and SPM flux and B) flux ratio of Chl-*a* to SPM. [a]x and y-axis for tide #2 set as (*1), compared to those in Figs. 3-5

As tide turned to offshore direction (stage-3), the Chl-*a* and SPM flux showed gradual increase in response to accelerating tidal current. Final stage-4 corresponds to mid-end of ebbing tide characterized by the decelerating tidal current thus resulted in decrease of the Chl-*a* and SPM flux accordingly.

Flux for Group II Data

Chl-*a* and SPM flux during the high tidal current and high wind speed period showed more strong relationship than those during the high current and low wind speed period (Fig. 3). In general, their fluxes increased about twice due to the strong wind effect (3-5 m s^{-1}) but this resulted in stronger coupling behavior of Chl-*a* and SPM during the submergence. For example, Chl-*a* and SPM flux for tide #5 showed similar temporal trends during the submergence and strong correlation was found at each stage of tidal current. Accordingly, there was no clear decoupling behavior of Chl-*a* from SPM at stage-2. There are 4 tides belonging to Group II condition and none of those showed the decoupling of Chl-*a* at stage-2, thus apparently high wind condition seemed not to allow the segregation of Chl-*a* from SPM at this time.

Flux for Group III Data

Nine out of 28 tidal cycles have been grouped into the low tidal energy period of which both current velocity (neap) and wind speed (mostly 0-1 m s^{-1}) are very weak. Due to the reduced tidal energy, the Chl-*a* and SPM flux considerably decreased by 10-fold (Fig. 4) compared to high tidal energy period (i.e., Group I-II; Figs. 2-3).

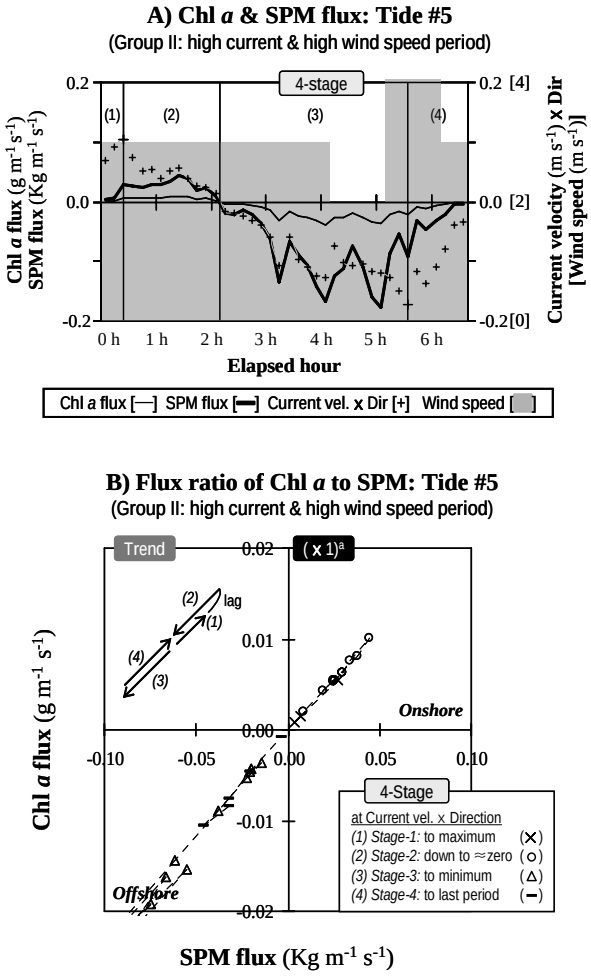

Fig. 3 Chl-*a* and SPM flux during period of high current (spring) and high wind speed (>2 m s^{-1}); example of tide #5 (categorized to Group II; tide #5, 24, 25, and 26), showing A) Chl-*a* and SPM flux and B) flux ratio of Chl-*a* to SPM. [a]x and y-axis (*1) same as those for tide #2 in Fig. 2

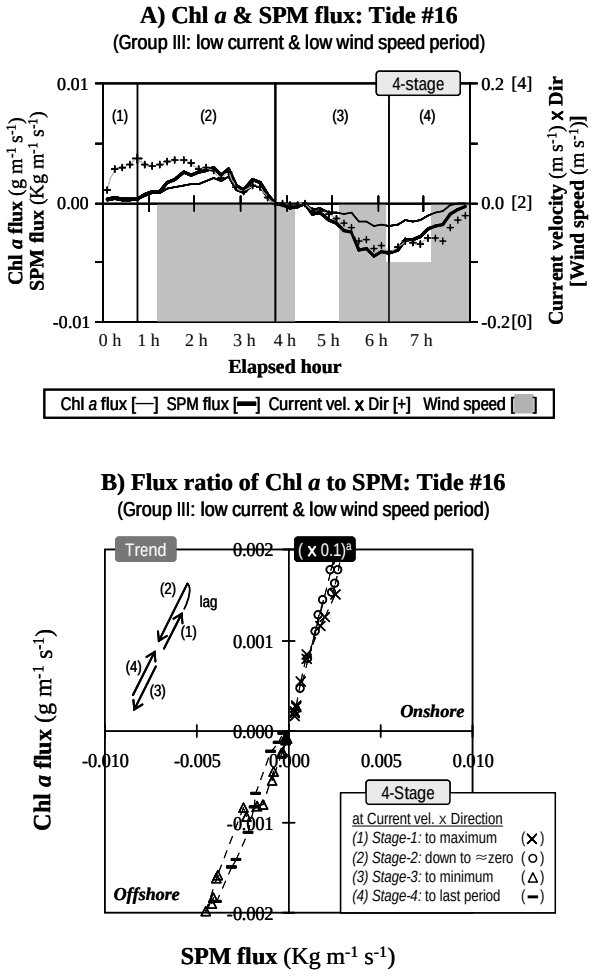

Fig. 4 Chl-*a* and SPM flux during period of low current (neap) and low wind speed (<2 m s^{-1}); example of tide #16 (categorized to Group III; tide #8, 9, 10, 12, 14, 16, 18, 20, and 21), showing A) Chl-*a* and SPM flux and B) flux ratio of Chl-*a* to SPM. [a]x and y-axis 10 times lower (*0.1) than those for tide #2 in Fig. 2

Coupling behavior of Chl-*a* from SPM during this period could be observed, not as clear as the ones observed during the high current and low wind speed period though. The ratios of Chl-*a* to SPM flux at stages 2-3 during the low tidal energy period were much greater (ca. 4-times) than those at same stages under the high tidal energy condition, indicating slow settlement of Chl-*a* and/or low concentrations of heavy SPM under the calm condition.

Flux for Group IV Data

Final group represents the period of low tidal current (neap) and high wind speed (mostly 3-5 m s^{-1}) period including 5 tides out of 28 (Fig. 5). Due to the reduced current velocities, the Chl-*a* and SPM flux was approximately 5 times lower than those in high current periods (group 1-2). No regular temporal trends (i.e., irregular fluctuation) have been found for Chl-*a* and SPM flux under this condition.

Although the wind speed between group II and IV was similar (3-5 m s^{-1}), the Chl-*a* and SPM flux for group IV were significantly lower than those in group II. This result, in other words, indicated that the current velocity directly controls the strength of Chl-*a* and SPM flux and wind effect only control their flux in terms of irregular distribution.

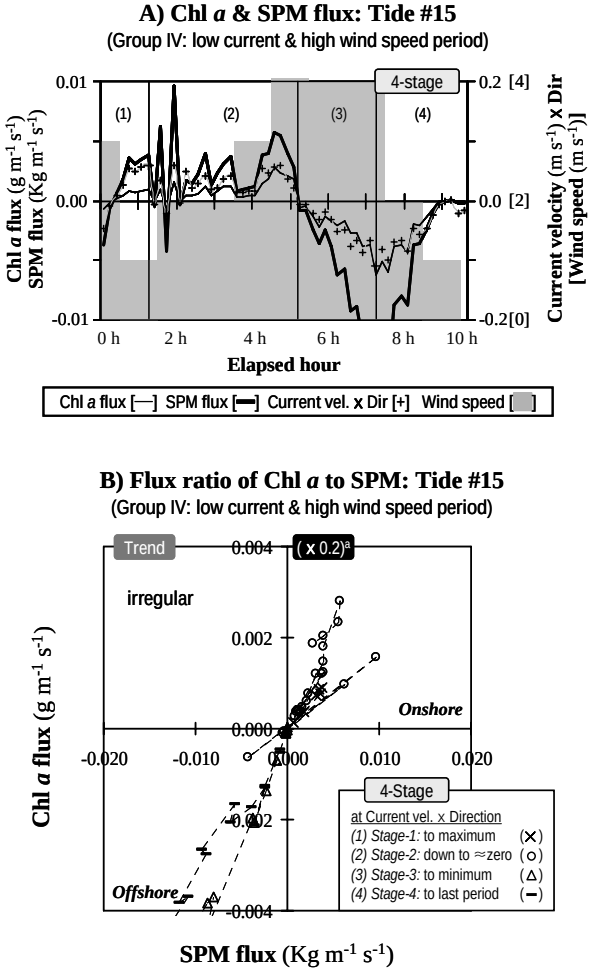

Fig. 5 Chl-*a* and SPM flux during period of low current (neap) and high wind speed (>2 m s^{-1}); example of tide #15 (categorized to Group IV; tide #11, 13, 15, 17, and 19), showing A) Chl-*a* and SPM flux and B) flux ratio of Chl-*a* to SPM. [a]x and y-axis 5 times lower (*0.2) than those for tide #2 in Fig. 2

DISCUSSION

Factors Controlling Chl-*a* and SPM Flux

In general, both the current velocity and wind speed influenced the temporal distribution and flux of the Chl-*a* and SPM during the course of resuspension followed by sedimentation in water column. However, the current velocity rather than wind speed was found to be the primary factor to control the strength of Chl-*a* and SPM flux. The wide range of flux variations during the spring tide was about 10-fold higher than that during the neap tide, on average, and this spring flux did not greatly differ regardless of wind strength (Figs. 2-3). While, the Chl-*a* and SPM flux decreased dramatically during the neap tide when the currently velocity decreased although the flux was slightly greater during the high wind period (Figs. 4-5). Apparently, wind itself did not influence the strength of Chl-*a* and SPM flux much but the strong wind still brought a large flux variation, thus both factors of the current velocity and wind speed are important to understand the Chl-*a* and SPM flux and their relationship in terms of tidal energy.

Segregation of Phyto-particles from SPM

Within the limited data though, we could find clear segregation of phyto-particles (Chl-*a*) from sediments (SPM) in water column, particularly during high current (spring) and low wind speed (<1.0 m s^{-1}) period. While, phyto-particles are strongly attached to the sediment particles during the all stages of low tidal energy (neap) period and stage 1, 3, and 4 of high tidal energy (spring) period. This phenomenon could be observed by looking at the Chl-*a* and SPM concentrations (further ratio of Chl-*a*/SPM) in water column during the flood-ebb tide as well (Koh et al. 2006). But the flux fitting of Chl-*a* to SPM at each stage more clearly showed the segregation phenomenon of phyto-particles from SPM (Fig. 2).

Overall, by examining the flux ratio of Chl-*a* to SPM, the couple of flux characteristics such as decoupling, flux

lag, and coupling mechanism between Chl-*a* and SPM in response to current velocity could be clearly observed. The segregated phyto-particles from SPM such as microphytobenthos would be important and could be one of the significant primary producers at certain periods, thus the understanding of particle dynamics would be highly beneficial (de Jonge 1992). However, it should be noted that this phenomenon was found based sorely on the single mooring data set for 15 days and may not be concluded as a general phenomenon. The in-depth analysis based on the plenty of data under the various tide conditions would be advanced for the further confirmation.

ACKNOWLEDGEMENTS

The study was conducted as part of the 'Research and Development Program' for New Bio-industry Initiatives (2001-03), Japan. This work was partly supported, during preparation of the manuscript, by the 2005 NLER Program, Ministry of Environment, Korea.

REFERENCES

Baillie, P.W. and Welsh, B.L. (1980) The effect of tidal resuspension on the distribution of intertidal epipelic algae in an estuary. Est. Coast. Mar. Sci. 10:165-180.

Black, K.S. (1998) Suspended sediment dynamics and bed erosion in the high shore mudflat region of the Humber Estuary, UK. Mar. Pollut. Bull. 37: 122-133.

Blanchard, G.F., Guarini, J.M., Orvain, F. and Sauriau, P.G. (2001) Dynamic behaviour of benthic microalgal biomass in intertidal mudflats. J. Exp. Mar. Bio. Eco. 264: 85-100.

de Jonge, V.N. (1995) Wind-driven tidal and annual gross transport of mud and microphytobenthos in the Ems Estuary, and its importance for the ecosystem, p. 29-40. In K.R. Dyer and R.J. Orth [eds.], Changes in fluxes in estuaries.

de Jonge, V.N. and van Beusekom, J.E.E. (1992) Contribution of resuspended microphytobenthos to total phytoplankton in the Ems estuary and its possible role for grazers. Neth. J. Sea. Res. 30: 91-105.

Koh, C.H., Khim, J.S., Araki, H., Yamanishi, H., Mogi, H. and Koga, K. (2006) Tidal resuspension of microphytobenthic chlorophyll *a* in Nanaura mudflat, Saga, Ariake Sea, Japan: Flood-ebb and spring-neap variations. Mar. Ecol. Pro. Ser. 312: 85-100.

Kuehl, S.A., Nittrouer, C.A., Allison, M.A., Ercilio, L., Faria, C., Dukat, D.A., Jaeger, J.M., Pacioni, T.D., Figueiredo, A.G. and Underkoffler, E.C. (1996) Sediment deposition, accumulation, and seabed dynamics in an energetic fine-grained coastal environment. Continen. Shelf. Res. 16: 787-815.

Smayda, T.J. (1974) Some experiments on the sinking characteristics of two freshwater diatom. Lim. Oceano. 19: 628-635.

Widdows, J., Blauw, A., Heip, G.H.R., Herman, P.M.J., Lucas, C.H., Middelburg, J.J., Schmidt, S., Brinsley, M.D., Twisk, F., Verbeek, H. (2004) Role of physical and biological processes in sediment dynamics of a tidal flat in Westerschelde Estuary, SW Netherlands Mar. Ecol. Pro. Ser. 274: 41–56.